Available online at www.sciencedirect.com

Chemical Engineering Research and Design

journal homepage: www.elsevier.com/locate/cherd

Novel approach to design and optimize heat-integrated distillation columns using Aspen Plus and an optimization algorithm

R. Gutiérrez-Guerra[a,*], J.G. Segovia-Hernández[b]

[a] Universidad Tecnológica de León, Campus I, Área de Sustentabilidad para el Desarrollo, Blvd. Universidad Tecnológica 225, Col. San Carlos, 37670 León, Gto., Mexico

[b] Universidad de Guanajuato, Campus Guanajuato, Departamento de Ingeniería Química, Noria Alta s/n, C.P., 36050 Guanajuato, Gto., Mexico

ARTICLE INFO

Article history:
Received 16 April 2023
Received in revised form 26 May 2023
Accepted 8 June 2023
Available online 10 June 2023

Keywords:
HIDiC configurations
Optimization
Purity constraint
Temperature driving forces
Aspen Plus

ABSTRACT

Heat-integrated distillation columns (HIDiC) are sustainable technologies whose optimized designs may reduce up 80% the energy consumption, cooling water and CO_2 emissions regard to the traditional columns. This paper shows a novel approach to design and optimize HIDiC columns using Aspen Plus and a stochastic optimization algorithm. This approach was designed to deal with the convergence problems in order to improve the search for the best solutions but also keep a continuous optimization process. The performance of the approach was evidenced through the optimization of the HIDiC columns used to split four close-boiling binary mixtures. Results showed that the design and optimization of these columns was successfully tackled by the approach implemented. As a result, the approach enabled to reduce convergence problems, keep a continuous optimization process and improve the quality of the solutions found. This fact demonstrates that the approach performed an adequate handling of purity specs and temperature driving forces, which were defined as constraints of the optimization problem. Based on the performance determined, this approach may be adapted and used as an approximated short-cut method to design and optimize other binary HIDiC columns. However, through an adequate adaptation, this approach may be extended to design and optimize HIDiC columns for separating ternary mixtures.

1. Introduction

Heat Integrated Distillation Columns (HIDiC) are environmentally friendly and energetically efficient and economically profitable configurations. In fact, reductions up 80% of the energy consumption, cooling water and carbon dioxide emissions, along with total annual costs reductions nearby to 18%, compared with the conventional columns, have been reported (Gutiérrez-Guerra et al., 2017). The flowsheet of the basic HIDiC configuration used to separate a feed stream into two products, bottoms (B) and dome (D), is depicted in Fig. 1.

The rectifying section (RS) is operated at higher pressure than the stripping section (SS). High pressure of RS is maintained using a centrifugal compressor (C) while low pressure of SS is kept using a throttling valve (TV). Thus, heat integration takes place from RS to SS considering the temperature driving forces allowed in the design and optimization problem of these configurations.

The design and operation characteristics that support the good performance of the HIDiC columns have been mainly

* Corresponding author.
E-mail address:
rogutierrez@utleon.edu.mx (R. Gutiérrez-Guerra).

https://doi.org/10.1016/j.cherd.2023.06.015

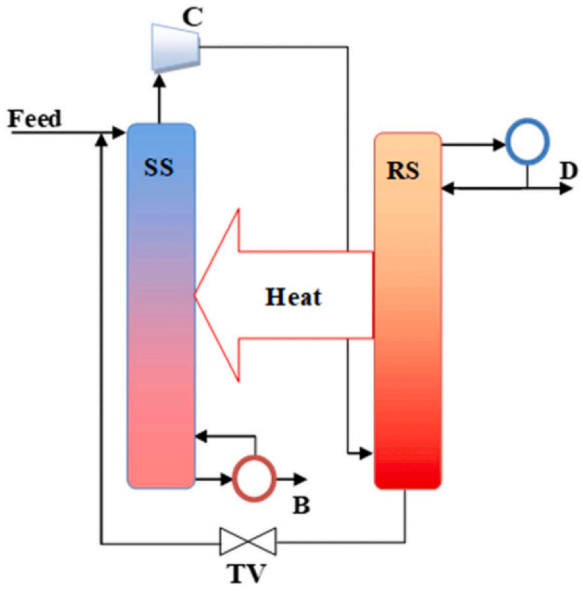

Fig. 1 – HIDiC configuration.

disclosed for continuous operation (Cong et al., 2017, Gadalla et al., 2007, Li et al., 2016, Marin-Gallego et al., 2022, Ponce et al., 2015, Seo et al., 2022, Suphanit, 2010, Wang et al., 2020). However, energetic benefits of some batch HIDiC columns have also been reported (Banerjee and Jana, 2017; Jana, 2016). Likewise, these intensified configurations have been subject to optimization studies through parametric analysis (Jana and Mali, 2010) and the implementation of optimization algorithms such as Genetic algorithms (GA) (Khalili et al., 2020, Qiu et al., 2019, Shahandeh et al., 2014), MINLP optimization (Harwardt et al., 2010) and the Boltzmann based estimation of distribution algorithm (Gutiérrez-Guerra et al., 2014, Gutiérrez-Guerra et al., 2016) and even the optimization using a combined approach, i.e., deterministic (MILP problem) and stochastic algorithms [simulated annealing algorithm (SA)] (Herrera Velázquez et al., 2022), and GA-PSO (particle swarm optimization) (Babaie and Nasr Esfahany, 2020) have been carried out.

The implementation of these approaches has revealed the most profitable economic and energetic performance of HIDiC configurations based on the kinds and features of the mixtures, optimal compression ratio, total number of stages, reflux ratio, heat distribution and heat transfer areas distribution, in addition to the most convenient structural configurations (e.g. concentric columns or arrangements with external heat transfer panels).

Besides, it is observed that the study of these configurations has mostly been addressed by simulation studies. Even, a considerable number of these studies was supported by process simulators (e.g. Aspen Plus) and the implementation of stochastic optimization algorithms.

However, despite there exist some basic systematic methodologies to design and optimize these configurations, no enough details have been disclosed to be considered as a standard method or short-cut method to track the design and optimization of these columns. Similarly, aspects related with the constraints handling [products purity, temperature driving forces (RS-SS)] and the modulation of the levels of heat integration of these configurations have not been completely addressed in explicit terms. In fact, most design and optimization studies simply indicate the target of purity, minimum temperature driving forces (RS-SS) allowed and calculations of heat to be integrated stage by stage. Nevertheless, neither explicit details about the method for the simultaneous handling of these constraints nor the influence among them are completely evidenced. Hence, the correlation among these constraints has not been disclosed on detail and its importance has not been highlighted for the optimization process in run time. In addition, in spite of HIDiC columns are complex structures, the inherent convergence problems and the approach to reduce them are not commonly disclosed in the papers published. However, these concerns represent a challenge yet to improve the optimization efficiency of these and other distillation configurations but also for other industrial processes. In fact, the study developed by Javaloyes-Antón et al. (2022) treats these kinds of concerns when process simulators (such as Aspen Plus) are used to optimize distillation columns. Similarly, Fu et al. (2015) carried out a complete Equation-Oriented Approach for Process Analysis and Optimization of a Cryogenic Air Separation Unit. In both cases, the models proposed tackled successfully the case studies analyzed. Also, Zhao et al. (2018) developed a superstructure optimization (MINLP) within the ProSimPlus Simulator. In this case, the main optimization process was performed by the simulator but the continuous and discrete variables were simultaneously optimized by an external metaheuristic algorithm (Mixed Integer Distributed Ant Colony Optimization). In addition, Hernández-Pérez et al. (2020) obtained favorable results through linking of the process simulator software Aspen Plus with a metaheuristic technique to optimize configurations for producing solar-grade silicon. Besides, Franke (2019) improved the convergence of an extractive distillation column using a Mixed-Integer optimization by connecting an external MINLP solver to Aspen Plus. Likewise, Seidel et al. (2020) developed a novel approach to optimize distillation columns. In this approach, the process simulation is embedded in the optimization problem and a small number of equations, constraints and optimization variables are defined. In comparison with the simulations using Aspen Plus, results show that the approach is a feasible alternative to perform the optimization of the distillation columns used as case studies.

Supported by the previous analysis, in this study an improved constrained design and optimization scheme for HIDiC configurations is presented. In this approach, Aspen Plus and a stochastic optimizer are linked each other through a correlation designed to relate the main design and optimization variables and the constraint handling.

This approach was developed to maintain a continuous (non-interrupted) optimization process through reducing the convergence problems that would be presented if typical design specs for purity were defined in Aspen Plus.

The evaluation of performance of the approach was based on the optimization of HIDiC columns using a Boltzmann based estimation of distribution algorithm recently published (Gutiérrez-Guerra et al., 2016). Although multiple HIDiC columns have been optimized using the principles of this approach, in this work the behavior of the approach was evidenced using four close-boiling equimolar mixtures, such as Cyclohexane/n-Heptane, Butanol/Isobutanol and Toluene/n-Octane and n-Octane/Ethylbencene.

The validation of the approach was performed taking as a reference the product purity constraints by executing simulations of Aspen Plus with design specs. These design specs

were implemented on hand by the user once the optimization process was concluded.

In general terms, this study shows the strengths of the approach but also underlines the numerical effort required. Furthermore, this scheme may be adapted to optimize the HIDiC configurations for other case studies due to the explicit structure of the approach.

2. Case studies

The performance of the approach presented in this work was determined for the HIDiC configurations optimized previously using a Bolztmann based estimation of distribution algorithm (Gutiérrez-Guerra et al., 2016). Particularly, four equimolar close-boiling mixtures were used as representative case studies. Each mixture was defined as follows: M1: Cyclohexane/n-Heptane, M2: Isobutanol/n-Butanol, M3: Toluene/n-Octane and M4: n-Octane/Ethylbenzene. A feed flow rate of 100 kmol/h was used for each mixture.

The Chao-Seader model was used to determine the thermodynamic properties of the mixtures M1, M3 and M4, while the thermodynamic properties of the mixture M2 were determined using the NRTL model. The selection of Chao-Seader was achieved because the corresponding mixtures are made of hydrocarbons, whereas M2 is a mixture made of alcohols (isomers of butanol) and it is well represented by the thermodynamic model proposed. In both cases, the recommendations given in Seader and Henley, 2006 were considered to employ the concerning thermodynamic models. In addition, the separation of the mixtures containing the kinds of alcohols used in this work has also been adequately performed using the NRTL model in other studies (e.g. Bastidas et al., 2012).

The minimization of the total annual cost (TAC) was established as the objective function of the optimization problem, using the compression ratio (CR), total number of stages (TNS) and reflux ratio (RR) as optimization variables of the problem. The purity (Xp) and recovery (Xr) of the products and the temperature driving forces ($\Delta T_{RS\text{-}SS}$, also called TDF) were defined as constraints of the problem. The design and operation features of the selected HIDiC designs for each mixture (obtained with the optimization carried before) and their respective conventional columns (CONV.), are presented in Table 1. RD and CD indicate the reboiler duty and compressor duty, respectively.

The HIDiC columns analyzed in this work were strategically selected to show the performance of the approach under several landscapes. For instance, behavior of the purity and temperature driving forces constraints considering reduction/increase of reflux ratio, variation of the heat integration due to the violation of temperature driving forces and reduction of the heat integration due to the limitations of the reflux ratio for accomplishing the purity constraint. Even, a particular case was chosen to show the simultaneous variation of these operation parameters.

3. Problem statement

3.1. *The first step of the approach is the establishment of the optimization problem*

In this case, the optimization performed using the Boltzmann based estimation of distribution algorithm was carried out for the optimization problem defined by Eq. (1) (Gutiérrez-Guerra et al., 2016).

$$\text{Min (TAC)} = f(\text{TNS}, \text{CR}, \text{RR}) \tag{1}$$

Subject to:

$$Xp = Xr = 0{\cdot}995 \pm \delta;\ \delta = 0{\cdot}0003 \text{ and } \Delta T_{RS\text{-}SS} \geq 1{\cdot}67\ \text{K}$$

Due to the fact that Xp≈Xr, this study is focused on the products purity, assuming the similar trend of the products recovery. The inherent relationship between both variables is justified because equimolar binary mixtures are used as case studies.

Furthermore, the TAC was evaluated using the method shown in the Appendix A of the supplementary material of this paper.

3.2. *In the second step the conceptual design of the HIDiC configurations is carried out*

In this case, the HIDiC configurations were designed by the optimizer with random values of TNS, CR and RR, considering the particular limits for the respective variable. Due to that the conventional columns were divided into two symmetrical sections, the feed stream was introduced in the first stage of SS of the HIDiC columns and the heat integration was made from RS to SS at stages located at the same level of both sections. Notice that reboiler and condenser were non-integrated stages.

3.3. *The third step is the calculation of the amount of integrated heat stage by stage*

Heat integration from RS to SS was carried out considering a proportional heat distribution according to the temperature driving forces between RS and SS (Suphanit, 2010), such as is shown in Eq. (2).

$$Q_i = \Delta T_{RSi-SSi}\left(\frac{Q_T}{\sum_{i=1}^{n}\Delta T_{RSi-SSi}}\right) \tag{2}$$

In this expression, i represents each stage of RS and SS, and n = TNS/2. Furthermore, QT and Qi were employed to indicate the total available amount of heat to be integrated and the amount of integrated heat per stage, respectively. QT is defined as the condenser duty of the non-optimized equivalent conventional configuration.

The condenser duty (QT) of the conventional column was used as the available heat to be transferred from the stages of RS to the stages of SS of the HIDiC configuration. In principle, this selection was made because the heat supplied to the reboiler of a conventional column is mostly rejected from the column to the environment through the cooling water used in the condenser. As a consequence, a low thermodynamic efficiency of these technologies of separation is determined. Therefore, through the heat integration performed in the HIDiC columns, energy recovery is achieved and the thermodynamic efficiency is improved.

At the same time, such as it was underlined by Kiss and Olujic', (2014), a more efficient energy usage is achieved when its distribution is made stage by stage instead to be supplied directly in the reboiler and removed in the condenser of the columns. This is the consequence of the heat

Table 1 – Case studies.

	M1		M2 (design 1)	
	HIDiC	Conv.	HIDiC	Conv.
TNS	44	44	72	72
RR	0.62	3.45	0.084	5.27
CR	1.95	-	1.76	-
Xr	0.9951	0.9948	0.9952	0.9952
Xp (mol frac.)	0.9951	0.9949	0.9950	0.9951
TAC (USD/y)	912402.42	623463.59	1164170.08	1180000.00
RD (kJ/h)	1579076.47	6704710.72	1043286.64	15815250.00
CD (kJ/h)	1034380.55	-	1153724.86	-
	M2 (design 2)		M3	
	HIDiC	Conv.	HIDiC	Conv.
TNS	80	80	72	72
RR	0.35	5.00	4.18	9.20
CR	1.75	-	1.29	-
Xr	0.9947	0.9949	0.9950	0.9953
Xp (mol frac.)	0.9947	0.9951	0.9950	0.9953
TAC (USD/y)	1200577.64	1179621.19	1527817.30	1508196.32
RD (kJ/h)	1665872.89	12368000.69	8023030.60	17205759.79
CD (kJ/h)	1063218.46	-	733201.66	-
	M4			
	HIDiC	Conv.		
TNS	86	86		
RR	8.64	18.80		
CR	1.39	-		
Xr	0.9948	0.9953		
Xp (mol frac.)	0.9947	0.9953		
TAC (USD/y)	2418673.30	2929527.00		
RD (kJ/h)	15181656.10	34621587.75		
CD (kJ/h)	1353634.43	-		

transfer at smaller temperature driving forces between the stages of RS and SS.

On the other hand, the non-optimized conventional columns used as base design to assemble the HIDiC columns were designed using a wide range of reflux ratio (1.5–25), Gutiérrez-Guerra et al., 2016. This range was established in order to generate higher duties in the condenser as the reflux ratio is increased. It is important to highlight that although a low RR (1.5) is used as lower limit, the optimization algorithm selects average values (or larger) of RR after evaluating the first generation of individuals (HIDiC designs). This behavior indicates that the conventional columns with low RR values do not generate HIDiC configurations with energetic benefits. Thus, RR values larger than the minimum reflux ratios required to satisfy the design specs of the conventional columns were used to design the equivalent HIDiC configurations. For instance, a minimum RR of 3.45 is required for reaching the design specs in the conventional column for the mixture made of Cyclohexane/n-Heptane. However, the equivalent HIDiC configuration was designed using a conventional column with RR of 5.50. Hence, larger RR values will produce higher condenser duties than the minimum reflux ratios required to meet the design specs of the conventional columns. Through this strategy, we have enough available heat to be integrated in the HIDiC columns.

Nevertheless, it is important to point out that the improvements given by the HIDiC configurations are determined by means of their comparison with the conventional columns with the same design specs.

It is important to point out that a similar approach was used in other studies to find the performance of the HIDiC columns and important benefits of the HIDiC columns were found (e.g. Suphanit, 2010).

3.4. *In the fourth step the heat integration is performed*

The heat integration is made in Aspen Plus using heat streams.

3.5. *In the fifth step the purity constraint handling is achieved*

Notice that once the heat integration (from RS to SS) is performed, considerably large purities (> 0.995) of both products are commonly obtained. Then, purity is reduced through the reduction of reflux ratio. However, as reflux ratio reduces, purity could fall below the target and an augment of reflux ratio must be achieved. In the first case (reflux ratio reduction), both reboiler duty and compressor duty of the HIDiC column are reduced. The contrary effect is experienced by the reboiler duty and compressor duty in the second case (increasing of reflux ratio).

Thus, the challenge is the dynamic modulation of reflux ratio (either reduction or increment) for meeting the product purity constraints, considering the temperature driving forces and the heat integration and other design and operation variables. Therefore, the simultaneous correlation of the constraints (purity and TDF), level of heat integration and other critical variables (such as TNS) is considered through the reflux ratio.

In a first instance, this problem could be tracked using design specs in the simulations of Aspen Plus. Nonetheless,

Table 2 – Correlation for modulation of reflux ratio in run time, Template of Excel. [representative cases for M1, M2 (design 1) and M3].

	M1							
	A	B	C	D	E	F	G	H
1	TNS/2:	RR:	HR:	XpLC:	XpHC:	Target:	TP1:	TP2:
2	22	5.50	0.97	0.9994	0.9995	0.995	0.4	120
3	Average factor:	WFP	FNS1:	FNS2:	Dif. XpLC:	Dif. XpHC:	1.25	70
4	= (E4 + F4)/2	=IF(A4 < 0;ABS(A4);A4)	=IF(A2 > =20;G2;G3)	=IF(A2 > =20;H2;H3)	=F2-D2	=F2-E2		
5	**RRnew:**	**=IF(A4 < 0;B2-B2 *B4 *C2 *C4 *D4;B2 +B2 *B4 *C2 *C4 *D4)**						
	M2(design 1)							
	A	B	C	D	E	F	G	H
1	TNS/2:	RR:	HR:	XpLC:	XpHC:	Target:	TP1:	TP2:
2	36	6.516	1.00	1.00	0.9998	0.995	0.25	90
3	Average factor:	WFP	FNS1:	FNS2:	Dif. XpLC:	Dif. XpHC:	0.3	85
4	= (E4 + F4)/2	=IF(A4 < 0;ABS(A4);A4)	=IF(A2 > =34;G2;G3)	=IF(A2 > =34;H2;H3)	=F2-D2	=F2-E2		
5	**RRnew:**	**=IF(A4 < 0;B2-B2 *B4 *C2 *C4 *D4;B2 +B2 *B4 *C2 *C4 *D4)**						
	M3							
	A	B	C	D	E	F	G	H
1	TNS/2:	RR:	HR:	XpLC:	XpHC:	Target:	TP1:	TP2:
2	36	13.00	0.99	0.9986	0.9988	0.995	0.25	80
3	Average factor:	WFP	FNS1:	FNS2:	Dif. XpLC:	Dif. XpHC:	0.4	90
4	= (E4 + F4)/2	=IF(A4 < 0;ABS(A4);A4)	=IF(A2 > =34;G2;G3)	=IF(A2 > =34;H2;H3)	=F2-D2	=F2-E2		
5	**RRnew:**	**=IF(A4 < 0;B2-B2 *B4 *C2 *C4 *D4;B2 +B2 *B4 *C2 *C4 *D4)**						

this option is not convenient in the optimization process because it is required to define lower and upper limits of the reflux ratio for each simulation in run time. This is a concern because initial reflux ratio values are so diverse that convergence problems are expected and consequent interruptions of the optimization process and loss of good individuals (designs) would be experienced.

On the other hand, when the modulation of reflux ratio is not enough to accomplish with the purity constraint, the optimization algorithm reduces the amount of integrated heat from RS to SS. Notice that such action cannot be performed through the typical design specs defined in Aspen Plus.

Therefore, instead of defining design specs in Aspen Plus, this problem is tackled by implementing a correlation to modulate the reflux ratio using the design and operation variables of the HIDiC columns. Particularly, the heat integration was explicitly considered in the math function of the approach, but the temperature driving forces are also considered in an implicit way. This fact is underlined due to that they represent the fundamental variables that support the performance of these configurations.

The correlation was assembled as a function in Excel for each mixture, such as it is shown in the Cell B5 of Table 2. Available data obtained in the optimization process were introduced for each design, but the execution of calculations has not been carried out in the template. Instead, referenced calculations are indicated in the corresponding cells. It is made with the aim to show the functioning of the approach (step by step) and users being able to extend it to other particular case studies.

Mole fraction is used as unity for light component purity (XpLC), heavy component purity (XpHC) and purity target.

The correlation was built considering each fundamental variable used to design and optimize HIDiC columns, such as it was underlined before.

The definition of each term of this function is described below:

RRnew (cell B5) is the new value of reflux ratio computed. Notice that the first condition (of B5) is performed when products purities are larger than the target (A4 < 0) and reflux ratio must be reduced. Otherwise, the second condition is performed. Here, the reflux ratio must be increased because a purity less than the target (i.e., A4 > 0) is experienced. Latter condition is included due to that the reductions of reflux ratio or reductions in the amount of integrated heat could lead to lower purities than the target and an augment of the reflux ratio must be achieved.

So, each RRnew calculated with the correlation is taken by Aspen Plus to perform the simulation of the corresponding HIDiC designs.

RR (cell B2) is the current reflux ratio.

HR (Cell C2) is defined as the heat ratio (HR), i.e., HR= (IH)/(RD + CD). Hence, HR represents the ratio of the integrated heat (IH) and the externally required energy (RD plus CD). This could be considered as the factor with the largest weight on the correlation due to that it meets the effect of the most important optimization variable of these columns, i.e., the compression ratio. This variable shows the highest impact in energetic and economic terms of these configurations, reason by which it has been the main optimization variable of the HIDiC columns.

The weight factor by purity (WFP) is used to consider the level of deviation of the current purity (regard the target of purity) in the correlation. This factor is computed as an average value of the differences of the purity for the light component (Dif. XpLC) and heavy component (Dif. XpHC), in relation with the purity target established. So, a larger WFP will have higher influence on the correlation. WFP is handled as a positive value in the correlation. This condition is required because the increase or reduction of reflux ratio is mathematically given by the corresponding sign, either - or

Table 3 – Calculation of reflux ratio for the second iteration of the HIDiC design, M1.

	A	B	C	D	E	F	G	H
1	TNS/2:	RR:	HR:	XpLC:	XpHC:	Target:	TP1:	TP2:
2	22	5.50	0.97	0.9994	0.9995	0.995	0.4	120
3	Average factor:	WFP	FNS1:	FNS2:	Dif. XpLC:	Dif. XpHC:	1.25	70
4	-0.004462	0.004462	0.4	120	-0.004396	-0.004528		
5	**RRnew:**	**4.36**						

+ (B2-B2…; B2 +B2…) included in the correlation. Therefore, additional negative signs must be avoided.

FNS1(C4) and FNS2 (D4) are factors related with the influence of the number of stages. The values taken by FNS1 and FNS2 are given by the couple of tuned parameters (TP1 and TP2). Therefore, the selection of each pair of values of these parameters depends on the number of stages of the columns, such as it is shown in the templates.

Table 2 shows that the same correlation was used to perform the purity adjustment of each HIDiC configuration for the respective mixture. Nonetheless, particular factors (TP1 and TP2) must be determined for each mixture due to that, as it was described, they depend on the number of stages.

Hence, it is evident that the correlation presented get together the effects of the set of fundamental design and operation variables of the HIDiC configurations, such as CR, TNS and RR. Of course, these variables are directly related with purity constraint and temperature driving forces.

Besides, although the general optimization was achieved by the Boltzmann based estimation of distribution algorithm, it is clear that a nested optimization is carried out to modulate the reflux ratio and meet the product purity through an effective constraint handling.

As an illustrative case, Table 3 shows the reflux ratio of the second iteration for the HIDiC design of M1 by executing the template shown in Table 2. Notice that each cell of Excel is filled with the corresponding data and the automatic execution of the template is performed. The reflux ratio calculated (RRnew= 4.361) can be verified in the further analysis for M1.

Similar calculations can be carried out for additional iterations of other HIDiC designs of the same mixture (M1) or for HIDiC designs of the other mixtures (M2, M3 and M4). Notice that RRnew depends on RR, HR, XpLC and XpHC of the previous iteration. Users must introduce the values in the cells of the corresponding mixtures (i.e., cells B2:E2) in the sheet of Excel, using the data presented in the section of results. The other parameters remain unchangeable. Users should follow the example shown in Table 3 (M1) for this purpose.

The overall optimization scheme is shown in Fig. 2. The first part (Part A) of the flowsheet is controlled by the optimizer while the second part (Part B) is handled by the correlation. So, the optimizer generates the population (HIDiC designs) of each generation, since the initial population (Po) to population Pt. Then, HIDiC designs are simulated in Aspen Plus and the product purity and temperature driving forces constraints are treated by the correlation. As a result, the penalized TAC is the output variable of the optimization process. The loop 1 (controlled by $N1 \leq NEiL1$) is used to perform the adjust of purity using the modulation of the reflux ratio only. So, the execution of this loop is stopped when the product purity is within the threshold (δ) or the number of evaluations (N1) is larger than the evaluations number of reflux ratio allowed per individual in loop 1 (NEiL1). The loop 2 (controlled by $N2 \leq NEiL2$) is implemented to reduce the amount of integrated heat when purity adjustment is not achieved using the reflux ratio only in the loop 1. In this case, an internal condition (XpLC-Target > 0.002) is considered. This condition indicates that if the difference between the current purity and purity target is lower than 0.002, purity continues to be adjusted using reflux ratio only. Otherwise, if the difference is larger than 0.002, IH must be reduced. In this case, depending on the particular mixture, IH is reduced with a factor between 10% and 15%, range found to be an appropriate reduction factor for IH for the mixtures examined. This percentage is applied as reduction factor for each heat-integrated stage. As an illustrative case, in this flowchart a reduction factor of 15% [using its equivalent reduction value (0.85) as operational factor] was applied. Notice that this kind of particular strategy to regulate the heat integration level has not been used in other studies of design and optimization of HIDiC configurations. However,

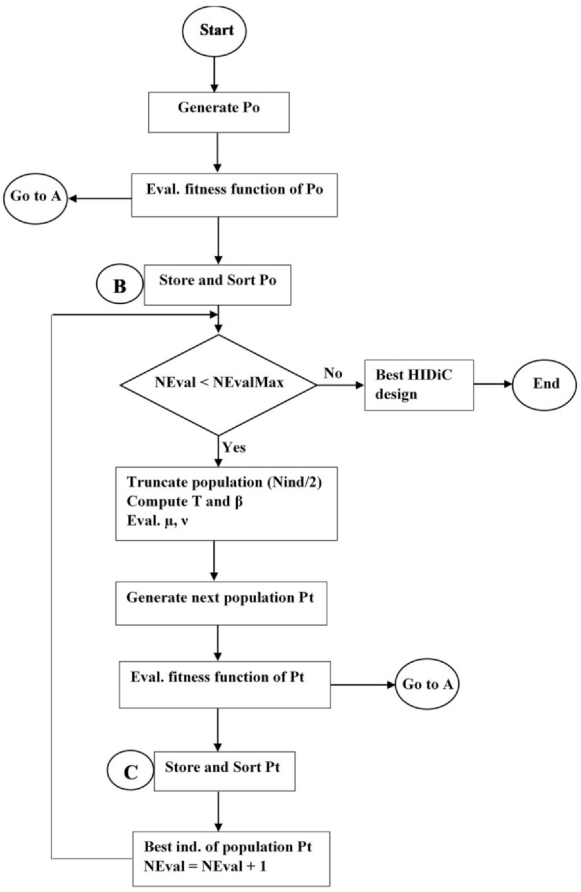

Fig. 2 – Approach of design and optimization of the HIDiC configurations (Part A). Fig. 2. Approach of design and optimization of the HIDiC configurations (Part B).

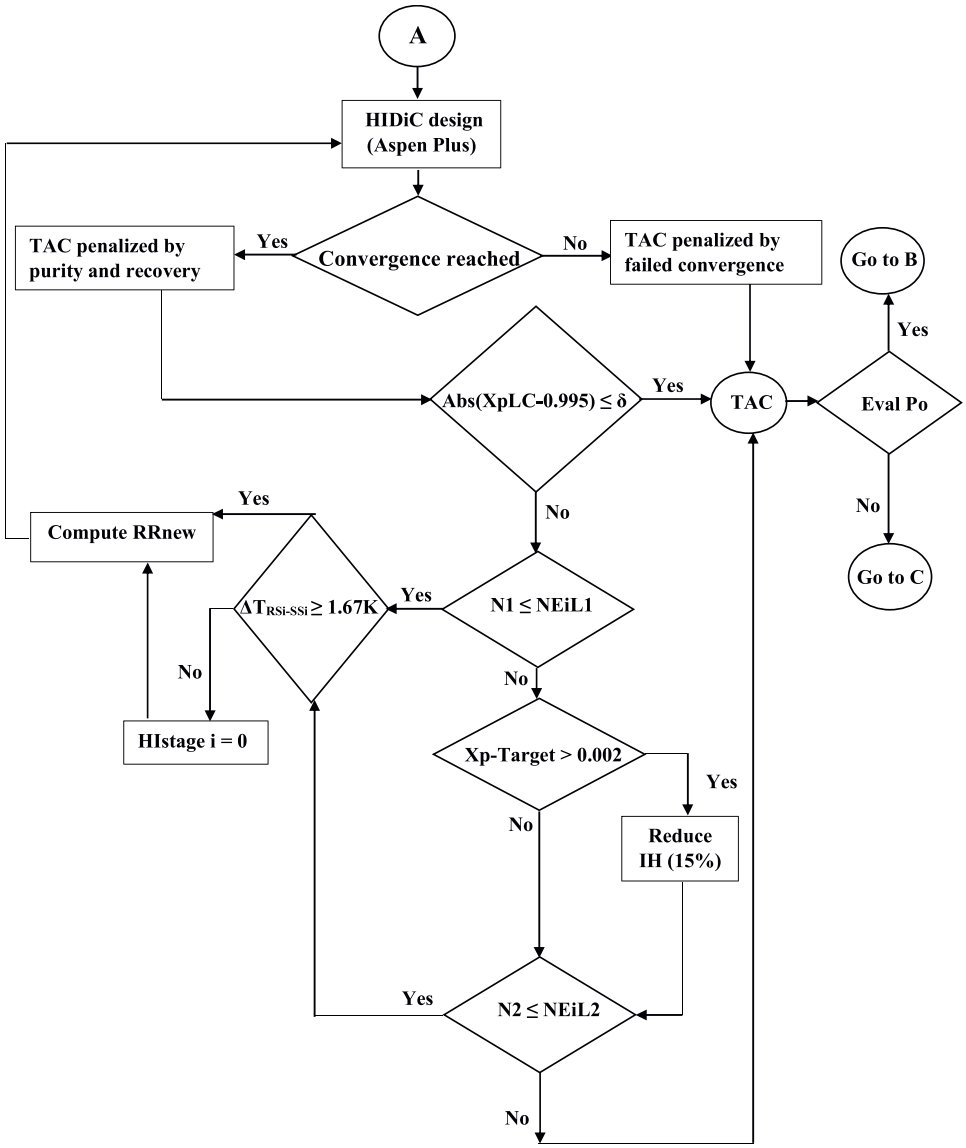

Fig. 2 – *(continued)*

this is a valuable method to control the temperature driving forces and the heat distribution in the stages of the columns. Accordingly, this control method helps to avoid the unnecessary complete suppression of the heat integration (Qi.=0) in the stages of the column throughout the product purity adjustment.

In this case, 45 total evaluations per individual (HIDiC design) were allowed considering both loops (loop 1 and loop 2) for the mixtures under study.

It is important to point out that regardless the process followed for the purity adjustment (either reflux ratio only or IH reduction, or both), the temperature driving forces are revised (and updated) for each evaluation of RRnew. Hence, any stage with $\Delta T_{RSi\text{-}SSi} < 1.67$ K is left without heat integration (IHstage i = 0). Therefore, IH reductions shown in this work might be a consequence of either the reduction factor (10–15%) or the violation of the temperature driving forces allowed.

On the other side, notice that the penalized TAC (fitness function) of each individual (HIDiC design) is taken, stored and ranked by the Boltzmann based estimation of distribution algorithm. Then, the optimizer uses the half of the current population with the best fitness function to produce the next generation of individuals (HIDiC designs).

Strictly speaking, the penalization of the TAC takes place only when the purity (and recovery) constraint established are violated, i.e., the purity is out of the threshold defined. In other words, the individuals that meet the constraints of purity (and recovery) have null penalization of the TAC.

Furthermore, when the convergence of the simulation is not achieved, an automatic large value (1E+09) is given to the TAC of that individual.

In summarized way (and for illustrative terms), a simplified fragment of the penalization approach established in Gutiérrez-Guerra et al. (2016) is given by Eqs. (3–5):

If the convergence of the simulation is true, Then.

$$TAC_{purity} = TAC + W_{purity} * TAC \quad (3)$$

$$TAC_{recovery} = TAC + W_{recovery} * TAC \quad (4)$$

where $W_{purity} = W_{recovery} = f * (XpLC\text{-}0.995)^2$ and f= 10.

$$TAC_{penalized} = TAC_{purity} + TAC_{recovery} \quad (5)$$

Else.

$TAC_{penalized}$=1E+09

End If.

Fig. 3 – Data flow in the optimization of the HIDiC columns.

The kind of penalization shown is named as weighting penalty. The weighted factor (f) was established after a trial and error process.

The terms T, β, ν and μ shown in the flowsheet are particular factors required by the optimizer, whose meaning and description might be found at Gutiérrez-Guerra et al., 2016.

On the other hand, the optimization process of the HIDiC columns shown in Fig. 2 is assisted by the process presented in Fig. 3. The process starts with the generation of the population by the optimizer in Matlab. This population is sent to Aspen Plus through Excel to be evaluated. Once the simulation is performed, results of the simulation are returned to excel where the fitness function is evaluated. Then, the fitness function value is sent to the optimizer. This optimization loop is executed until the optimization process is completed.

4. Results and discussion

The optimization results of the HIDiC columns obtained with the approach presented are shown in Tables 4–11.

Results show that a gradual reduction of the purity (Tables 4–6) is experienced through modulated changes of the reflux ratio induced by the correlation developed, until reaching the purity constraint established in the optimization process. Furthermore, the high level of numerical precision of the correlation is evidenced with the step size of the reflux ratio experienced from one iteration to another, such a way that relatively large step changes were experienced at beginning of the purity adjustment, but they were gradually reduced for evaluations nearby to the purity target established. This fact demonstrates the inherent relationship between both variables (reflux ratio and purity) and how the correlation handles it successfully.

On the other hand, it is also evidenced a continuous reduction of the reboiler duty and compressor duty (Tables 4–6). This is a consequence of less liquid flow to be vaporized in the reboiler and less steam to be compressed with the compressor. So, due to that the integrated heat remains constant along the process [at least for M1 and M2 (design 1)], the heat ratio is continuously increased. The constant value of the heat integration indicates that feasible temperature driving forces between stages of RS and SS were preserved along the process of purity adjustment. Notice that although a variable amount of heat integration is experienced by M3, the trend of the continuous increment of HR was also experienced by this mixture. This behavior demonstrates the influence of the reflux ratio, modulated by the correlation, on HR. At the same time, it is observed that the fitness function of the problem (TAC) gradually decreases until a minimum value is obtained. Hence, the relatively large initial values of the TAC indicate higher level of penalization due to that the purity constraint is out of the threshold established. Thus, this penalization reduces as purity adjustment proceeds, getting zero penalization when the final purity lies within the threshold defined. As it is observed, the final TAC of each HIDiC design is taken by the Boltzmann based estimation of distribution algorithm to conduct the optimization of these configurations considering the characteristics of the best individuals to generate each new population.

These outcomes prove the useful work achieved by the correlation (attached to the optimization algorithm) to perform the modulation of the reflux ratio to meet the purity constraint. The result of RRnew of the second iteration (shown in Table 4) can be corroborated with the calculations carried out in Table 2 and Table 3, for M1.

On the other hand, as described before, there exist cases of HIDiC configurations that might experience non-feasible temperature driving forces in some stages and no heat integration is carried out in such stages. Therefore, the total IH decreases further as a larger number of stages violates the temperature constraint. Notice that although this fact takes place, the reflux ratio is simultaneously modulated. This behavior is shown in Table 6. As it is observed, IH undergoes a continuous reduction as the purity approximates to the target established.

With the aim to support the behavior shown in Table 6, Table 7 shows some illustrative cases (iterations) that evidence the reduction of IH (as a function of the temperature driving force per stage) as purity adjustment proceeds. Notice that the non-integrated stages were not included in Table 7. As it is observed, the heat integration of 20 stages was performed in the first iteration but the number of heat integrated stages reduces for further iterations. In fact, 15 heat integrated stages were determined in iteration 3 and only 11 stages were integrated for the final HIDIC design of this configuration. As it was mentioned before, this trend is a

Table 4 – Purity adjustment for the HIDiC design of M1 (TNS=44, CR=1.95).

RR	XpLC (mol frac.)	XpHC (mol frac.)	HR	IH (kJ/h)	CD (kJ/h)	RD (kJ/h)	TAC (USD/y)
5.50	0.9994	0.9995	0.97	9188262.32	1664242.42	7850750.7	1632027.76
4.36	0.9992	0.9994	1.16	9188262.32	1517663.64	6389468.64	1474304.91
3.32	0.9988	0.9991	1.43	9188262.32	1383611.03	5055910.12	1311689.46
2.42	0.9983	0.9986	1.78	9188262.32	1266952.57	3893672.74	1184886.36
1.70	0.9976	0.9978	2.22	9188262.32	1174450.53	2972797.55	1084166.47
1.21	0.9969	0.9967	2.66	9188262.32	1110833.79	2337884.56	1013923.58
0.93	0.9962	0.9960	3.01	9188262.32	1074897.25	1980860.67	974873.55
0.78	0.9958	0.9955	3.23	9188262.32	1055718.52	1790089.41	935149.02
0.71	0.9954	0.9954	3.36	9188262.32	1045691.21	1691483.83	924711.93
0.66	0.9953	0.9951	3.44	9188262.32	1039541.96	1629617.22	917606.06
0.64	0.9952	0.9952	3.48	9188262.32	1036677.15	1601904.76	914909.99
0.62	0.9951	0.9951	3.52	9188262.32	1034380.55	1579076.47	912402.42

Table 5 – Purity adjustment for the HIDiC design of M2 (Design 1, TNS=72, CR=1.76).

RR	XpLC (mol frac.)	XpHC (mol frac.)	HR	IH (kJ/h)	CD (kJ/h)	RD (kJ/h)	TAC (USD/y)
6.516	1.0000	0.9998	1.00	15026765.60	2000678.02	13058481.36	2428147.07
5.800	1.0000	0.9997	1.10	15026765.60	1905691.96	11721655.22	2297561.83
5.101	1.0000	0.9996	1.23	15026765.60	1812864.83	10415619.81	2150348.54
4.423	1.0000	0.9996	1.38	15026765.60	1725668.34	9146799.46	2028547.20
3.766	0.9999	0.9998	1.57	15026765.60	1653122.31	7909507.73	1918218.82
3.117	0.9998	0.9998	1.82	15026765.60	1565711.38	6699160.41	1794471.52
2.504	0.9998	0.9996	2.14	15026765.60	1482163.37	5553038.25	1658090.41
1.937	0.9995	0.9995	2.55	15026765.60	1405704.37	4496496.34	1548846.60
1.436	0.9994	0.9990	3.07	15026765.60	1337467.28	3563481.02	1455830.00
1.017	0.9987	0.9987	3.70	15026765.60	1281050.93	2783342.24	1372871.65
0.706	0.9978	0.9982	4.37	15026765.60	1238849.01	2201566.75	1311368.24
0.499	0.9976	0.9973	4.96	15026765.60	1210737.94	1816885.01	1272112.62
0.363	0.9966	0.9970	5.45	15026765.60	1192359.56	1563520.79	1219748.25
0.284	0.9962	0.9966	5.78	15026765.60	1181662.99	1416842	1204151.80
0.233	0.9959	0.9963	6.02	15026765.60	1174720.93	1321562.88	1193961.94
0.198	0.9957	0.9961	6.19	15026765.60	1169996.95	1256660.27	1187053.90
0.173	0.9958	0.9958	6.32	15026765.60	1166585.92	1210182.91	1182458.86
0.153	0.9956	0.9957	6.43	15026765.60	1163905.16	1173179.81	1178271.36
0.139	0.9954	0.9957	6.51	15026765.60	1161951.77	1146290.33	1175278.73
0.128	0.9953	0.9956	6.57	15026765.60	1160470.32	1125829.73	1172948.19
0.119	0.9953	0.9955	6.62	15026765.60	1159315.1	1110234.22	1171454.55
0.112	0.9951	0.9955	6.67	15026765.60	1158315.84	1096301.52	1169724.84
0.106	0.9952	0.9954	6.70	15026765.60	1157559.38	1086083.15	1168768.61
0.101	0.9951	0.9954	6.73	15026765.60	1156886.43	1076658.27	1167651.75
0.097	0.9951	0.9954	6.75	15026765.60	1156341.32	1069208.06	1166858.73
0.094	0.9951	0.9954	6.77	15026765.60	1155869.59	1062756.38	1166171.72
0.091	0.9950	0.9954	6.79	15026765.60	1155458.23	1057129.93	1165572.19
0.088	0.9950	0.9953	6.81	15026765.60	1155097.37	1052194.14	1165045.95
0.086	0.9950	0.9953	6.82	15026765.60	1154779.16	1047841.48	1164581.65
0.084	0.9950	0.9953	6.84	15026765.60	1153724.86	1043286.64	1164170.08

Table 6 – Purity adjustment for the HIDiC design of M3 (TNS=72, CR=1.29).

RR	XpLC (mol frac.)	XpHC (mol frac.)	HR	IH (kJ/h)	CD (kJ/h)	RD (kJ/h)	TAC (USD/y)
13.00	0.9986	0.9988	0.99	23101261.97	1622669.23	21700381.60	3059123.55
12.05	0.9984	0.9986	1.00	21695901.52	1517760.41	20239482.58	2886262.01
11.21	0.9984	0.9983	1.07	21695901.52	1469331.46	18903509.04	2777419.38
10.42	0.9983	0.9981	1.14	21695901.52	1423106.98	17633948.09	2676624.37
9.67	0.9982	0.9979	1.22	21695901.52	1379219.15	16430221.79	2581650.02
8.96	0.9981	0.9980	1.30	21695901.52	1338470.99	15310602.85	2497761.16
8.25	0.9979	0.9981	1.40	21695901.52	1297401.4	14184732.28	2417294.56
7.55	0.9978	0.9976	1.45	20812717.11	1225556.14	13097430.12	2289577.31
6.96	0.9976	0.9977	1.56	20812717.11	1191714.42	12168300.67	2224171.78
6.39	0.9975	0.9974	1.68	20812717.11	1158284.99	11251187.25	2159504.02
5.86	0.9973	0.9974	1.72	19857862.24	1094283.25	10450262.75	2022776.11
5.39	0.9970	0.9970	1.75	18853868.24	1031696.10	9736222.60	1933137.27
5.00	0.9968	0.9967	1.76	17815997.98	972699.03	9156401.05	1813407.50
4.70	0.9965	0.9965	1.74	16754574.55	917816.81	8711355.37	1746908.45
4.46	0.9962	0.9961	1.70	15676583.79	865720.12	8360603.88	1686706.75
4.29	0.9958	0.9958	1.63	14586755.19	817600.08	8128579.89	1633810.67
4.18	0.9950	0.9950	1.41	12383328.88	733201.66	8023030.60	1527817.30

consequence of the behavior of the temperature driving forces due to the influence of the reflux ratio reductions for a constant CR. Consequently, this strong influence of the reflux ratio justifies the consideration of this variable in the optimization of HIDiC columns and the important work carried out by the correlation is demonstrated.

On the other side, Table 8 shows three consecutive IH reductions (10–15%) for the HIDiC configurations of M4. This behavior takes place because the purity adjustment was not reached with the reflux ratio modulation only. The first one reduction is observed at IH= 32989544.50 kJ/h, the second one reduction was for IH= 27936208.00 kJ/h and the third one reduction was carried out at IH= 20041181.10 kJ/h, which gave as a result 12195391.50 kJ/h. It is important to underline that, after the first reduction, a dynamic reduction factor for IH is performed for next consecutive iterations while the difference between the current purity and target is out of the minimum value established (0.002). Therefore, IH reductions were performed as follows:

First IH reduction: IHnew1 = (0.995/ XpLC)*IH* 0.85.

Second IH reduction: IHnew2 = (0.995/ XpLC)*IHnew1 * 0.85 * 0.85.

Table 7 – Behavior of the heat integration with the reduction of the reflux ratio for M3 (TNS=72, CR=1.29).

	RR= 10.42		RR= 7.55		RR= 4.70		RR= 4.18	
Stage	IH (kJ/h)	TDF (K)	IH (KJ/h)	TDF (K)	IH (kJ/h)	TDF (K)	IH (kJ/h)	TDF (K)
2	1139664.43	4.97	1139664.43	4.78	1139664.43	4.30	1139664.43	3.79
3	1136914.04	4.93	1136914.04	4.72	1136914.04	4.19	1136914.04	3.63
4	1134211.92	4.87	1134211.92	4.66	1134211.92	4.08	1134211.92	3.44
5	1131546.27	4.82	1131546.27	4.59	1131546.27	3.95	1131546.27	3.23
6	1128897.92	4.77	1128897.92	4.51	1128897.92	3.81	1128897.92	3.01
7	1126236.3	4.71	1126236.3	4.43	1126236.3	3.65	1126236.3	2.76
8	1123514.88	4.64	1123514.88	4.35	1123514.88	3.48	1123514.88	2.49
9	1120663.16	4.58	1120663.16	4.25	1120663.16	3.28	1120663.16	2.20
10	1117576.37	4.50	1117576.37	4.15	1117576.37	3.07	1117576.37	1.93
11	1114099.43	4.42	1114099.43	4.04	1114099.43	2.83	1114099.43	1.78
12	1110004.16	4.33	1110004.16	3.92	1110004.16	2.57	1110004.16	1.67
13	1104956.8	4.24	1104956.8	3.78	1104956.8	2.30		
14	1098469.45	4.12	1098469.45	3.62	1098469.45	2.02		
15	1089828.68	3.99	1089828.68	3.45	1089828.68	1.76		
16	1077990.72	3.84	1077990.72	3.24	1077990.72	1.68		
17	1061423.47	3.65	1061423.47	3.01				
18	1037870.2	3.41	1037870.2	2.73				
19	1003994.04	3.11	1003994.04	2.40				
20	954854.86	2.72	954854.86	2.00				
21	883184.41	2.19						

Third IH reduction: IHnew3 = (0.995/ XpLC)*IHnew2 * 0.85 * 0.85 * 0.85.

The complete calculation for the first IH reduction is given by:

IHnew1 = (0.995/0.9987)* (32989544.50)* 0.85 = 27937225.65 kJ/h.

The other reductions can be computed in a similar way.

Particularly, a specific reduction factor of 15% was applied for this mixture. Hence, the equivalent factor used is given as 0.85.

Notice that a deviation between the calculated value and reported value is expected due to the rounding of significant digits for the purity in Table 8.

To corroborate the data presented in Table 8, Table 9 shows the temperature driving forces and the heat integration at each stage. As it can be seen, the heat integration was kept at all stages for the illustrative reflux ratio values. Thus, these results evidence that feasible temperature driving forces were produced in the stages shown for this HIDiC configuration. Therefore, the variation of IH per stage is a consequence of the reduction factor (15%) described before, but not due to infeasible temperature driving forces. As before, the non-integrated stages were not included in Table 9.

In a complementary analysis, the HIDiC design shown in Table 10 experiences simultaneous variation of the parameters described before. In this case, the reflux ratio undergoes both reduction (starting at 7.36) and increasing (starting at reflux ratio of 0.02) along the purity adjustment process. In addition, this HIDiC column experiences IH reductions (observed at reflux ratio of 0.01) because of the violation of temperature driving forces and also reductions using the reduction factor of 15% described before (observed at reflux ratio of 0.01).

Thus, the approach implemented to deal with the constraints in the rigorous optimization of HIDiC columns demonstrates its capability for handling multiple parameters in a simultaneous way.

On the other hand, a particular analysis of the results depicted in Table 6, Table 8 and Table 10 evidences variable amounts of heat integration for the corresponding mixtures. This behavior conducts to establish that the implementation of the typical design specs in Aspen Plus is not possible for these mixtures because from one simulation to another (either reduction or increasing of reflux ratio) infeasible temperature driving forces for some stages are experienced or the reduction of IH is performed. This is established due to the fact that the typical design specs defined in Aspen Plus do not treat with the heat integration. Consequently, the convergence would not be reached for these designs. Considering this fact, it is interesting to point out that if the design specs were defined in Aspen Plus, the best HIDiC design found for M3 but also good HIDiC designs for the other mixtures would be lost.

Based on the previous analysis, it is evident that the successful convergence of the simulations in Aspen Plus with design specs depends on a constant amount of integrated heat. However, the correlation itself is implicitly constituted by IH and works with variable heat integration, which supports its better performance in relation with the establishment of design specs in the simulations of Aspen Plus under the proposed optimization scheme. So, taking into account that the heat integration is the core of the HIDiC configurations, the optimization performed using the correlation coupled to the optimizer makes possible to obtain the great energy savings using these configurations.

With the aim to validate the results obtained through the approach presented, the HIDiC designs of some representative cases were compared with the results determined using design specs in the simulations of Aspen Plus for the cases of constant heat integration. The comparative analysis is presented in Table 11, while the evaluation procedure for each individual using design specs is shown in the Appendix B of the supplementary material of this paper.

Results of Table 11 shows that the purity adjustment using reflux ratio (modulated by the correlation) was reached using 12 iterations (M1) whereas the purity constraint was reached using 18 iterations by defining design specs in Aspen plus. The adjusting of purity for the mixture M2 (design 1) required 30 iterations for both cases (using the correlation and design specs in Aspen Plus). Notice that data for the HIDiC columns of the mixtures M2(design 2), M3 and M4 were

Table 8 – Purity adjustment for the HIDiC design of M4 (TNS=86, CR=1.39).

RR	XpLC (mol frac.)	XpHC (mol frac.)	HR	IH (kJ/h)	CD (kJ/h)	RD (kJ/h)	TAC (USD/y)
20.92	0.9991	0.9996	0.95	35640166.50	3454796.60	33986839.20	4818441.18
20.15	0.9991	0.9995	0.91	32989544.50	3267397.05	32855031.60	4624191.16
19.45	0.9991	0.9985	0.94	32989544.50	3211189.62	31724994.80	4498696.56
18.84	0.9990	0.9994	0.97	32989544.50	3161078.68	30715862.70	4427216.12
18.16	0.9990	0.9991	1.01	32989544.50	3106337.16	29611888.20	4322713.33
17.50	0.9990	0.9990	1.04	32989544.50	3053705.88	28555980.20	4226145.85
16.86	0.9989	0.9995	1.08	32989544.50	3004793.58	27575420.10	4158928.96
16.19	0.9989	0.9987	1.12	32989544.50	2949549.41	26456325.70	4036027.62
15.58	0.9988	0.9995	1.16	32989544.50	2898932.03	25438593.40	3973861.64
14.92	0.9988	0.9994	1.21	32989544.50	2845273.59	24358768.20	3872062.60
14.26	0.9987	0.9994	1.26	32989544.50	2793417.33	23314006.40	3784006.46
12.21	0.9983	0.9986	1.24	27936208.00	2388424.39	20223157.40	3345781.15
9.44	0.9971	0.9968	1.12	20041181.10	1790397.24	16102878.40	2742995.70
6.69	0.9924	0.9925	0.92	12195391.50	1196173.33	12025687.80	2091888.77
6.83	0.9926	0.9928	0.91	12195391.50	1207310.59	12248656.60	2111294.71
6.95	0.9928	0.9931	0.89	12195391.50	1217416.38	12451158.20	2129013.92
7.07	0.9929	0.9933	0.88	12195391.50	1226631.33	12635681.00	2145353.02
7.17	0.9931	0.9935	0.87	12195391.50	1234913.68	12801752.90	2159893.70
7.27	0.9932	0.9936	0.86	12195391.50	1242566.46	12955232.40	2173350.63
7.35	0.9933	0.9936	0.85	12195391.50	1249576.31	13096058.30	2185472.67
7.44	0.9934	0.9937	0.84	12195391.50	1256501.80	13234827.00	2247522.12
7.52	0.9935	0.9934	0.83	12195391.50	1262919.38	13362927.40	2258326.95
7.60	0.9936	0.9938	0.83	12195391.50	1269968.84	13504412.10	2271002.96
7.67	0.9937	0.9937	0.82	12195391.50	1275563.31	13616646.70	2280776.43
7.75	0.9938	0.9940	0.81	12195391.50	1281444.56	13734433.70	2291361.99
7.81	0.9939	0.9942	0.81	12195391.50	1286320.64	13831460.20	2300099.15
7.86	0.9939	0.9940	0.80	12195391.50	1290586.95	13917536.70	2307190.56
7.92	0.9940	0.9941	0.80	12195391.50	1295213.55	14009978.80	2315598.92
7.97	0.9941	0.9941	0.79	12195391.50	1299476.85	14095677.00	2322803.88
8.02	0.9941	0.9938	0.79	12195391.50	1303487.21	14177382.00	2329709.08
8.08	0.9942	0.9946	0.78	12195391.50	1308339.33	14274259.70	2338999.64
8.12	0.9942	0.9945	0.78	12195391.50	1311386.41	14334510.50	2344234.13
8.15	0.9942	0.9943	0.78	12195391.50	1314107.45	14389136.20	2348747.77
8.19	0.9943	0.9938	0.77	12195391.50	1317537.19	14457478.00	2354293.83
8.25	0.9943	0.9945	0.77	12195391.50	1321834.12	14543890.70	2362606.30
8.28	0.9944	0.9945	0.77	12195391.50	1324364.36	14594657.10	2366978.14
8.31	0.9944	0.9940	0.76	12195391.50	1326909.62	14646705.10	2370837.54
8.35	0.9944	0.9942	0.76	12195391.50	1330153.50	14711659.90	2376892.20
8.39	0.9945	0.9940	0.76	12195391.50	1333360.89	14775915.40	2382208.21
8.43	0.9945	0.9944	0.75	12195391.50	1336914.83	14846811.90	2388730.23
8.47	0.9945	0.9947	0.75	12195391.50	1339492.05	14898311.90	2393788.06
8.49	0.9946	0.9947	0.75	12195391.50	1341252.35	14933332.50	2396826.02
8.51	0.9946	0.9946	0.75	12195391.50	1342823.22	14964936.20	2399464.26
8.53	0.9946	0.9951	0.75	12195391.50	1344554.86	14999618.20	2402990.65
8.54	0.9946	0.9945	0.75	12195391.50	1345365.32	15015888.60	2403856.90
8.56	0.9946	0.9944	0.74	12195391.50	1347411.99	15056986.10	2407283.64
8.59	0.9947	0.9947	0.74	12195391.50	1349618.37	15101136.00	2411553.85
8.61	0.9947	0.9948	0.74	12195391.50	1351052.82	15129885.90	2414128.80
8.63	0.9947	0.9948	0.74	12195391.50	1352367.10	15156242.10	2416440.65
8.64	0.9947	0.9948	0.74	12195391.50	1353634.43	15181656.10	2418673.30

no compared because the implementation of design specs was not achieved due to the variable heat integration from one simulation to another for these HIDiC columns.

It is important to mention that each simulation using design specs was run such as it was originally designed by the optimization algorithm (without purity adjustment), only design specs (lower and upper reflux ratio values and purity target) were defined by user. If simulation converges, results are saved. Otherwise, if the simulation does not get convergence with the current parameters (lower and upper limit of reflux ratio) of design specs, these values are modified and the simulation is performed again. Notice that when the convergence is not reached in the first run (or previous run), the simulation is reinitialized before proving next lower and upper limits of reflux ratio. This action is made with the aim to avoid guidance of the simulator on results of the first simulation (or previous simulation). Of course, the convergence and iterations number will depend on the values of the limits established for reflux ratio and the step size of the increments used from one reflux ratio to another. Nonetheless, is not a goal of this work to show the optimal number of iterations when design specs are implemented in the simulation. At the same time, if simulations with design specs were executed in run time of the optimizer, the aim would be the adjustment of the purity instead to minimize the internal iterations in Aspen Plus to evaluate design specs. Besides, the comparison is considered acceptable due to that the optimization algorithm also works with certain grade of

Table 9 – Heat integration reduction for the HIDiC design of M4 (TNS=86, CR=1.39).

	RR= 14.26		RR= 12.21		RR= 9.44		RR= 6.69		RR= 8.64	
Stage	IH(kJ/h)	TDF(K)	IH (kJ/h)	TDF (K)	IH(kJ/h)	TDF(K)	IH(kJ/h)	TDF(K)	IH(kJ/h)	TDF(K)
2	1436826.61	7.54	1216733.59	7.41	872873.60	7.10	531158.08	6.57	531158.08	6.78
3	1432859.79	7.49	1213374.41	7.36	870463.75	7.05	529691.64	6.51	529691.64	6.73
4	1428807.86	7.44	1209943.16	7.30	868002.19	6.99	528193.75	6.45	528193.75	6.68
5	1424640.46	7.38	1206414.12	7.24	865470.49	6.93	526653.17	6.39	526653.17	6.62
6	1420320.86	7.32	1202756.2	7.19	862846.34	6.87	525056.32	6.33	525056.32	6.57
7	1415803.44	7.26	1198930.76	7.12	860102.00	6.81	523386.35	6.26	523386.35	6.51
8	1411025.62	7.19	1194884.8	7.06	857199.47	6.74	521620.11	6.19	521620.11	6.46
9	1405925.82	7.12	1190566.18	6.99	854101.33	6.67	519734.84	6.12	519734.84	6.40
10	1400412.98	7.04	1185897.8	6.91	850752.28	6.60	517696.89	6.05	517696.89	6.33
11	1394369.66	6.95	1180780.2	6.83	847080.96	6.52	515462.83	5.97	515462.83	6.27
12	1387659.61	6.85	1175098	6.75	843004.60	6.44	512982.30	5.89	512982.30	6.20
13	1380108.12	6.74	1168703.23	6.65	838417.05	6.35	510190.70	5.81	510190.70	6.13
14	1371496.31	6.62	1161410.59	6.55	833185.37	6.26	507007.13	5.72	507007.13	6.05
15	1361549.4	6.48	1152987.35	6.43	827142.62	6.15	503330.02	5.63	503330.02	5.97
16	1349921.55	6.32	1143140.64	6.30	820078.68	6.04	499031.50	5.53	499031.50	5.89
17	1336177.06	6.14	1131501.54	6.15	811728.89	5.92	493950.51	5.43	493950.51	5.80
18	1319765.44	5.92	1117603.86	5.98	801758.82	5.79	487883.56	5.31	487883.56	5.70
19	1299990.4	5.67	1100857.95	5.79	789745.46	5.64	480573.23	5.20	480573.23	5.58
20	1275971.74	5.37	1080518.47	5.57	775154.10	5.47	471694.14	5.07	471694.14	5.46
21	1246599.15	5.01	1055645.16	5.31	757310.22	5.28	460835.85	4.93	460835.85	5.32
22	1210481.44	4.59	1025059.96	5.00	735368.68	5.06	447484.05	4.78	447484.05	5.17
23	1165898.29	4.09	987306.05	4.65	708284.37	4.82	431002.80	4.61	431002.80	4.99
24	1110777.82	3.52	940628.94	4.23	674798.63	4.53	410626.17	4.43	410626.17	4.78
25	1042740.25	2.87	883013.36	3.75	633465.74	4.21	385474.42	4.22	385474.42	4.54
26	959285.16	2.18	812341.92	3.21	582766.69	3.83	354623.21	4.00	354623.21	4.26

randomness and user does not has intervention to intentionally guide the optimization process toward good solutions.

In terms of iterations number, data of Table 11 shows that the correlation experiences a comparable and even better performance that the simulations with design specs. Nevertheless, it is important to point out that each iteration achieved using design specs is performed in a single run of Aspen Plus (18 internal iterations are made for M1), whereas one run for each simulation is performed in Aspen Plus by

Table 10 – Integral performance of the HIDiC design for M2 (Design 2, TNS=80, CR=1.75).

RR	XpLC (mol frac.)	XpHC (mol frac.)	HR	IH (kJ/h)	CD (kJ/h)	RD (kJ/h)	TAC (USD/y)
8.29	1.0000	1.0000	1.00	18605441.70	2435391.46	16185151.90	2954720.13
7.36	1.0000	1.0000	1.11	18605441.70	2314765.31	14457159.60	2787770.06
6.44	1.0000	0.9999	1.25	18605441.70	2195045.64	12743764.70	2603653.59
5.55	1.0000	0.9999	1.42	18605441.70	2077557.77	11062337.30	2440176.05
4.67	1.0000	0.9999	1.64	18605441.70	1957992.71	9419794.22	2277821.71
3.82	1.0000	0.9998	1.92	18605441.70	1851925.31	7833972.79	2123942.86
3.01	1.0000	0.9996	2.31	18605441.70	1746192.36	6321113.12	1956096.77
2.26	1.0000	0.9995	2.84	18605441.70	1652582.11	4909162.42	1823197.19
1.58	1.0000	0.9995	3.59	18605441.70	1568495.31	3617024.06	1702882.24
0.98	0.9998	0.9996	4.67	18605441.70	1491414.17	2490004.42	1588949.73
0.49	0.9998	0.9992	6.17	18605441.70	1427607.85	1587961.47	1472482.80
0.19	0.9986	0.9992	7.74	18605441.70	1384131.40	1020510.71	1396753.40
0.06	0.9986	0.9990	8.65	18605441.70	1367698.13	783079.45	1374506.73
0.01	0.9981	0.9978	8.11	16683909.80	1235200.19	823114.78	1295062.86
0.01	0.9899	0.9896	6.56	13423251.50	1017504.52	1028115.57	1128737.42
0.01	0.9900	0.9896	6.54	13423251.50	1018044.58	1035625.16	1129600.22
0.02	0.9901	0.9898	6.49	13423251.50	1018987.46	1048724.28	1131112.92
0.03	0.9902	0.9901	6.42	13423251.50	1020653.41	1070940.55	1133493.49
0.05	0.9906	0.9905	6.30	13423251.50	1023298.25	1107853.09	1137716.52
0.08	0.9911	0.9910	6.12	13423251.50	1027387.96	1164698.41	1144091.57
0.12	0.9918	0.9918	5.89	13423251.50	1033084.36	1244527.61	1153123.61
0.17	0.9926	0.9926	5.64	13423251.50	1040024.11	1341434.43	1164157.43
0.23	0.9931	0.9933	5.40	13423251.50	1047073.66	1439893.90	1174734.93
0.28	0.9939	0.9939	5.19	13423251.50	1053710.83	1533345.30	1185537.14
0.31	0.9945	0.9943	5.05	13423251.50	1058511.65	1600090.93	1193363.60
0.34	0.9947	0.9946	4.97	13423251.50	1061426.48	1640840.00	1197967.59
0.35	0.9947	0.9948	4.92	13423251.50	1063218.46	1665872.89	1200577.64

each iteration using the correlation. In other words, 18 internal iterations are carried out in a single run of the simulation using design spec in Aspen Plus, but 12 runs are required to perform twelve simulations in Aspen Plus with the correlation. An analogous statement is also applied for the corresponding iterations number required for M2 (design 1).

Likewise, it is important to observe that similar final values of reflux ratio and reboiler duty were determined using the correlation and simulations with design specs, which led to very similar products purities in both cases for the HIDiC columns of the corresponding mixture.

Accordingly, it is shown that the implementation of design specs in Aspen Plus has a better behavior in the purity adjustment because multiple internal evaluations are performed in a single simulation. Nonetheless, as it was described before, the correlation allowed to reduce convergence problems and avoid the loss of good individuals along the optimization process when design specs are established in the simulations of Aspen Plus.

Thus, a better performance is obtained implementing the correlation in relation with the use of design specs in the simulations of Aspen Plus. This behavior takes place because the correlation relates the fundamental design and operation variables and the constraint handling in a simultaneous way along the optimization of HIDiC configurations.

The advantages of the correlation are highlighted because Aspen Plus does not has a default method for regulating the heat integration stage by stage considering the minimum temperature driving forces. In this case, such issue is tackled by the Boltzmann based estimation of distribution algorithm but it is also considered by the correlation implemented. So, user should create this structure as an internal routine in Aspen Plus (if such specific thing is possible in the simulator) to consider simultaneously this issue if design specs are defined in the simulation.

Hence, results presented validate the good performance of the correlation implemented, which is supported by next achievements:

a) Good control of the purity constraint and the modulation of the penalization of the fitness function (TAC) was achieved.
b) A fair comparison of performance of the HIDiC designs for the corresponding mixture was carried out because a comparable purity was determined among them.
c) Feasible temperature driving forces to perform the heat transfer from RS to SS were verified because they were implicitly revised in the approach for each reflux ratio.
d) Convergence problems expected when design specs are defined in Aspen Plus in run time of the optimization process were avoided.
e) Interruptions of the optimization process and loss of good individuals were eluded due to expected convergence problems for the simulations when design specs are defined in Aspen Plus.
f) The design and optimization scheme presented allowed to harness the huge potential of the interface between Aspen Plus, the correlation and the Boltzmann-based optimizer. So, this strategy tackles the design and optimization of the HIDiC columns through the coupling of the correlation of fundamental design and operation variables, rigorous simulations in Aspen Plus and a robust optimization process.

Notice however, that the performance of the HIDiC columns may also be determined through the adequate material and energy balances modeling and other relationships, along with the implementation of an optimizer. Nevertheless, the aim in this work is to take advantage of the robustness of Aspen Plus to perform rigorous simulations using the internal math methods for solving MESH equations in a more efficient way. Although, as has been emphasized, the simulations in Aspen Plus require the support of the correlation presented for the constraint handling and perform an adequate heat integration. The wide use of Aspen Plus to design and optimize HIDiC columns and other distillation configurations is evidenced in literature (Babaie et al., 2020, Cong et al., 2017, Herrera Velázquez et al., 2022, Li et al., 2016, Ponce et al., 2015, Qiu et al., 2019).

g) The nested optimization for purity constraint using reflux ratio as manipulated variable (through the correlation) enhances the main optimization loop (minimization of the TAC) performed by the Boltzmann based estimation of distribution algorithm. This is achieved because the individuals (HIDiC designs) with less deviation of the purity, regard the target established, will experience lower level of penalization or null penalization (when the purity is within the threshold defined). Thus, the optimization algorithm will identify the best individuals (lower fitness functions) in an easier way and will conduct the search for better solutions considering the characteristics of such individuals (HIDiC configurations).

Notice, however, that larger numerical effort and optimization time is expected to preserve the purity within the threshold established using the correlation, in comparison with the establishment of purity constraint handling as an inequality function (e.g. $Xp > 0.99$). In fact, the execution of the purity adjustment loop for each HIDiC design described before takes about 8 s per iteration. So, the total time will depend on the total iterations required for accomplishing the purity constraint.

It is important to point out that most of this time is used to perform the simulations of Aspen Plus and data transference between the interface given by Optimizer-Excel-Simulator but not in the optimization performed by the optimizer itself.

This estimation of time was determined by using an i5 processor core computer, clock frequency at 2.8 GHz and 16 GB of RAM, through the interface assembled with Matlab-Excel-Aspen Plus.

Hence, the cost-benefit disclosed supports the approach presented. By one side, the approach relates the fundamental variables of the HIDiC columns along with the constraints handling (through the correlation), but both considerable numerical effort and optimization time are required to perform a continuous robust optimization process.

However, it is important to underline that these optimizations were made using wide limits of the optimization variables, e.g., CR was evaluated from 1.1 to 10 (Gutiérrez-Guerra et al., 2016). Thus, optimization results allowed to find the most favorable values of the optimization variables of the best HIDiC designs, e.g. optimal $CR < 2.2$, for these close-boiling mixtures. Therefore, shorter limits for the process variables will be used in future optimization problems of these configurations. Consequently, the reduction in the limits of the optimization variables and enhancements in data transfer and computational resources will lead to meaningful reductions of numerical effort and computing time in subsequent optimization problems of HIDiC

Table 11 – Performance of the correlation vs. simulations with design specs.

	M1		M2 (design 1)	
	Correlation	Design specs	Correlation	Design specs
Iterations	12	18	30	30
RR	0.62	0.61	0.084	0.056
XpLC (mol frac.)	0.9951	0.9951	0.9950	0.9950
RD (kJ/h)	1579076.47	1563802.73	1043286.64	993462.75

configurations. These improvements will increase the strengths of this approach to optimize these intensified configurations.

5. Conclusions

In this paper a novel approach to design and optimize Heat-Integrated Distillation Columns using Aspen Plus and an optimization algorithm is presented.

The goal was to reduce the convergence problems of the simulations in Aspen Plus and keep a continuous optimization process. This is performed through the correlation of both design and operational variables along with the adequate constraint handling of these configurations. The approach was evaluated performing the separation of four close-boiling mixtures.

Results showed the adequate correlation of the optimization variables and constraints of these configurations through the approach implemented, which led to intensified searches through a continuous robust optimization process. The validation of the results was achieved by comparing the results obtained using the approach with those determined using design specs in Aspen Plus in suitable cases. The comparison showed that the purity was reached by the correlation in lower or similar number of iterations, in relation with the design specs defined in Aspen Plus, but longer simulation time was used by the correlation. However, the correlation showed advantages over using of design specs defined in the simulations of Aspen Plus. For instance, the reflux ratio is dynamically updated considering the integrated heat and number of stages through the correlation, which implicitly leads to update the temperature driving forces established in the optimization problem. Furthermore, despite both considerable computing time and numerical effort were determined in the optimization process achieved using the correlation, these concerns are alleviated using more efficient computing equipment, improvements in the data transfer between the simulator and optimizer and adequate definition of the limits for the optimization variables.

On other hand, it is evident the feasibility of extension of this approach to other case studies because the assembling of the correlation was explicitly described using referenced calculations though cells of Excel and each parameter of it was detailed.

So, supported by the findings disclosed, this novel approach provides important insights regard the design and optimization of the HIDiC columns. In fact, through adequate adaptation, this approach can be extended and coupled with other optimization algorithms, such as GA, PSO, SA, to optimize both binary and ternary HIDiC columns.

Declaration of Competing Interest

The authors declare that they have no known competing financial interests or personal relationships that could have appeared to influence the work reported in this paper.

Appendix A. Supporting information

Supplementary data associated with this article can be found in the online version at doi:10.1016/j.cherd.2023.06.015.

References

Babaie, O., Nasr Esfahany, M.N., 2020. Optimization and heat integration of hybrid R-HIDiC and pervaporation by combining GA and PSO algorithm in TAME synthesis. Sep. Purif. Tech. 236, 116288. https://doi.org/10.1016/j.seppur.2019.116288

Banerjee, S., Jana, A.K., 2017. Internally heat integrated batch distillation: Vapor recompression and nonlinear control. Sep. Pur. Tech. 189, 267–278. https://doi.org/10.1016/j.seppur.2017.08.003

Bastidas, P., Parra, J., Gil, I., Rodriguez, G., 2012. Alcohol distillation plant simulation: thermal and hydraulic studies. Proc. Eng. 42, 80–89. https://doi.org/10.1016/j.proeng.2012.07.397.

Cong, H., Li, X., Li, H., Murphy, J.P., Gao, X., 2017. Performance analysis and structural optimization of multi-tube type heat integrated distillation column (HIDiC). Sep. Pur. Tech. 188, 303–315. https://doi.org/10.1016/j.seppur.2017.07.047

Franke, M.B., 2019. Mixed-integer optimization of distillation sequences with Aspen Plus: a practical approach. Comp. Chem. Eng. 131 (5), 106583. https://doi.org/10.1016/j.compchemeng.2019.106583

Fu, Q., Zhu, L., Chen, X., 2015. Complete equation-oriented approach for process analysis and optimization of a cryogenic air separation unit. Ind. Eng. Chem. Res. 2015 (54), 12096–12107. https://doi.org/10.1021/acs.iecr.5b02768

Gadalla, M., Jiménez, L., Olujic', Z., Jansens, P.J., 2007. A thermo-hydraulic approach to conceptual design of an internally heat-integrated distillation column (iHIDiC). Comput. Chem. Eng. 31, 1346–1354. https://doi.org/10.1016/j.compchemeng.2006.11.006

Gutiérrez-Guerra, R., Cortez-González, J., Murrieta-Dueñas, R., Segovia-Hernández, J.G., Hernández, S., Hernández-Aguirre, A., 2014. Design and optimization of heat-integrated distillation column schemes through a new robust methodology coupled with a Boltzmann-based estimation of distribution algorithm. Ind. Eng. Chem. Res. 53, 11061–11073. https://doi.org/10.1021/ie500084w

Gutiérrez-Guerra, R., Murrieta-Dueñas, R., Cortez-González, J., Segovia-Hernández, J.G., Hernández, S., Hernández-Aguirre, A., 2016. Design and optimization of HIDiC columns using a constrained Boltzmann-based estimation of distribution algorithm-evaluating the effect of relative volatility. Chem. Eng. Proc. 104, 29–42. https://doi.org/10.1016/j.cep.2016.02.004

Gutiérrez-Guerra, R., Murrieta-Dueñas, R., Cortez-González, J., Segovia-Hernández, J.G., Hernández, S., Hernández-Aguirre,

A., 2017. Design and optimization of heat-integrated distillation configurations with variable feed composition by using a Boltzmann-based estimation of distribution algorithm as optimizer. Chem. Eng. Res. Des. 124, 46–57. https://doi.org/10.1016/j.cherd.2017.05.025

Harwardt, A., Kraemer, K., Marquardt, W., 2010. Identifying optimal mixture properties for HIDiC application. Proceedings of Distillation and Absorption 2010;55–60.

Hernández-Pérez, L.G., Ramírez-Márquez, C., Segovia-Hernández, J.G., Ponce-Ortega, J.M., 2020. Simultaneous structural and operating optimization of process flowsheets combining process simulators and metaheuristic techniques: the case of solar-grade silicon process. Comput. Chem. Eng. 140 (2), 106946. https://doi.org/10.1016/j.compchemeng.2020.106946

Herrera Velázquez, J.J., Zavala Durán, F.M., Chavez Díaz, L.A., Cabrera Ruiz, J., Alcantara Avila, J.R., 2022. Hybrid two-step optimization of internally heat-integrated distillation columns. J. T. Inst. Chem. Eng. 130, 1–9. https://doi.org/10.1016/j.jtice.2021.06.061

Jana, A.K., 2016. New divided-wall heat integrated distillation column (HIDiC) for batch processing: feasibility and analysis. App. Energy 172, 199–206. https://doi.org/10.1016/j.apenergy.2016.03.117

Jana, A.K., Mali, S.V., 2010. Analysis and control of a partially heat integrated refinery debutanizer. Comput. Chem. Eng. 34, 1296–1305. https://doi.org/10.1016/j.compchemeng.2010.03.002

Javaloyes-Antón, J., Kronqvist, J., Caballero, J.A., 2022. Simulation-based optimization of distillation processes using an extended cutting plane algorithm. Comput. Chem. Eng. 159, 107655. https://doi.org/10.1016/j.compchemeng.2021.107655

Khalili, N., Kasiri, N., Ivakpour, J., Khalili-Garakani, A., Khanof, M.H., 2020. Optimal configuration of ternary distillation columns using heat integration with external heat exchangers. Energy 191, 1–12. https://doi.org/10.1016/j.energy.2019.116479

Kiss, A.A., Olujic', Z., 2014. A review on process intensification in internally heat-integrated distillation columns. Chem. Eng. Proc. 86, 125–144 http://dx.doi.org/10.1016/j.cep.2014.10.017.

Li, H., Cong, H., Li, X., Li, X., Gao, X., 2016. Systematic design of the integrating heat pump into heat integrated distillation column for recovering energy. Appl. Therm. Eng. 105, 93–104. https://doi.org/10.1016/j.applthermaleng.2016.05.141

Marin-Gallego, M., Mizzi, B., Rouzineau, D., Gourdon, C., Meyer, M., 2022. Concentric Heat Integrated Distillation Column (HIDiC): a new specific packing design, characterization and pre-industrial pilot unit validation. Chem. Eng. Proc. 171, 108643. https://doi.org/10.1016/j.cep.2021.108643

Ponce, S.F.G.H., Alves, M., Miranda, J.C.C., Rubens Maciel, F., Wolf Maciel, M.R., 2015. Using an internally heat-integrated distillation column for ethanol–water separation for fuel applications. Chem. Eng. Res. Des. 95, 55–63. https://doi.org/10.1016/j.cherd.2015.01.002

Qiu, P., Huang, B., Dai, Z., Wang, F., 2019. Data-driven analysis and optimization of externally heat-integrated distillation columns (EHIDiC). Energy 189, 116177. https://doi.org/10.1016/j.energy.2019.116177

Seader, J.D., Henley, E., 2006. Separation Process Principles. John Wiley and Sons, New York.

Seidel, T., Hoffmann, A., Bortz, M., Scherrer, A., Burger, J., Asprion, N., Küfer, K.-H., Hasse, H., 2020. A novel approach for infeasible path optimization of distillation-based flowsheets. Chem. Eng. Sci.: X 7, 100063. https://doi.org/10.1016/j.cesx.2020.100063

Seo, C., Lee, H., Lee, M., Lee, J.W., 2022. Energy efficient design through structural variations of complex heat-integrated azeotropic distillation of acetone-chloroform-water system. J. Ind. Eng. Chem. 109, 306–319. https://doi.org/10.1016/j.jiec.2022.02.012

Shahandeh, H., Ivakpour, J., Kasiri, N., 2014. Internal and external HIDiCs (heat integrated distillation columns) optimization by genetic algorithm. Energy 64, 875–886. https://doi.org/10.1016/j.energy.2013.10.042

Suphanit, B., 2010. Design of internally heat-integrated distillation column (HIDiC): uniform heat transfer area versus uniform heat distribution. Energy 35, 1505–1514.

Wang, Z., Qin, W., Yang, C., Wang, W., Xu, S., Gui, W., Sun, Y., Xie, D., Wang, Y., Lu, J., Chen, Q., Liu, X., 2020. Heat-transfer distribution optimization for the heat-integrated air separation column. Sep. Purif. Tech. 248, 117048. https://doi.org/10.1016/j.seppur.2020.117048

Zhao, Q., Neveux, T., Mecheri, M., Privat, R., Guittard, P., Jaubert, J.N., 2018. Superstructure optimization (MINLP) within ProSimPlus simulator. Comp. AidChem. Eng. 43, 767–772. https://doi.org/10.1016/B978-0-444-64235-6.50135-2